Eur. Phys. J. D **8**, 153–156 (2000)

THE EUROPEAN PHYSICAL JOURNAL D

EDP Sciences

Rapid Note

Laser energy deposition in relativistic interactions with underdense plasmas

P. Chessa[1], M. Galimberti[1,2], A. Giulietti[1], D. Giulietti[1,2], L.A. Gizzi[1,a], and P. Mora[3]

[1] Istituto di Fisica Atomica e Molecolare, Via del Giardino 7, 56127 Pisa, Italy
[2] Dipartimento di Fisica, Università di Pisa, and INFM, Italy
[3] Centre de Physique Théorique, École Polytechnique, 91128 Palaiseau Cedex, France

Received 28 September 1999 and Received in final form 26 October 1999

Abstract. It is well established that, at sub-relativistic intensities, the absorption of laser light by underdense plasmas decreases with increasing pulse intensity as interaction enters a non-linear regime. On the other hand, as the relativistic interaction regime is reached, further absorption mechanisms can be activated which can account for a substantial energy transfer. Using the particle code WAKE, we performed numerical simulations of the relativistic interaction of intense laser pulses with underdense plasmas in conditions that can be experimentally tested. Our simulations show that, while the relativistic laser intensity generates a population of *fast* electrons, a considerable fraction of the pulse energy goes into a population of *thermal* electrons. These findings open new possibilities for a direct observation of relativistic interaction processes using high resolution soft X-ray techniques.

PACS. 52.50.Jm Plasma production and heating by laser beams – 52.40.Nk Laser-plasma interactions (e.g., anomalous absorption, backscattering, magnetic field generation, fast particle generation) – 52.25.Rv Emission, absorption, and scattering of visible and infrared radiation

At moderate laser intensities, the absorption of a laser pulse propagating in a long-scale underdense plasma takes place mostly *via* collisional inverse bremsstrahlung (IB) absorption. However, as the laser intensity increases, the electron quivering velocity also increases, the IB process becomes non-linear [1] (and references therein) leading to lower levels of absorption [2]. The situation changes completely when the laser intensity enters the relativistic regime and almost all the energy of the laser pulse can be deposited in the plasma [3]. This energy goes into wakefields and fast electrons and can be transferred to ions during the process of plasma channelling. All these processes are typical features of relativistic interactions [4].

A way to assess the importance of relativistic effects is to consider the normalized relativistic momentum, $a_0 = p_{\rm os}/m_0 c \approx 0.85\,\lambda_0 I_{\rm L}^{1/2}$ where $p_{\rm os}$ is the momentum of the electrons oscillating in the laser field, m_0 is the electron mass, c is the speed of light, and $I_{\rm L}$ and λ_0 are the laser intensity in units of 10^{18} W/cm^2 and the wavelength in micrometers, respectively. When the $a_0 > 1$ relativistic effects start to become important. Although this is a regime of enormous interest, no detailed studies of the absolute laser energy deposition into the plasma have been carried out so far, neither numerically, nor experimentally. Generally, it is simply assumed that in relativistic conditions most of the deposited energy goes into fast electrons. Accordingly, the experiments in this field are based upon measurements on electrons, ions or photons of high energy which escape from the interaction region. These measurements are used to obtain information on self-focusing conditions or accelerating fields in laser-plasma channels [5]. Some experimental data also exist which provide an estimate of the energy deposited in a plasma channel [6] and the residual transmitted pulse energy [7,8].

An open question is whether in laser interactions at relativistic intensities there is still an important fraction of the so-called *thermalised* electrons, that is, electrons whose typical kinetic energies are sufficiently low to allow collisional processes to play a role in the excitation and decay of ions and in particular in radiation emission processes. This does not necessarily mean that the entire electron population is described by a Maxwellian distribution function, but only that the usual equilibrium models, namely coronal or collisional-radiative equilibrium can be applied to the study of radiation emission processes. In this sense, we will refer to these electrons as *thermalised*. The presence of these electrons may have relevant experimental implications, making it possible to use, in relativistic interaction experiments, highly advanced soft-X-ray diagnostics typically used in non-relativistic experiments [9–11], allowing a more accurate study of the interaction physics. Laser self-focusing or plasma channelling, for example, could be detected directly using high-resolution soft X-ray techniques successfully used in a previous

[a] e-mail: leo@ifam.pi.cnr.it

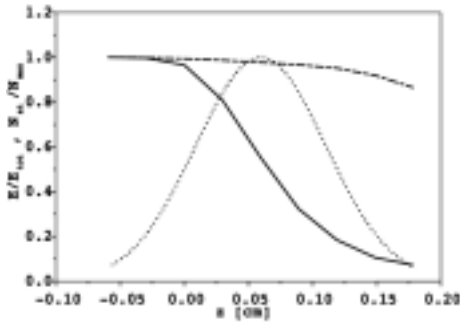

Fig. 1. Laser energy reaching a given plane $z = const$ as a function of the distance along the propagation axis for two laser intensities: of 3×10^{18} W/cm^2 (solid line) and 4×10^{17} W/cm^2 (dashed line). The atomic density distribution (dotted line) of the gas-jet target is also plotted. The laser pulse propagates from left to right. The focal plane in vacuum corresponds to $z = 0$ where the atomic density is $N = N_{\max}/2$.

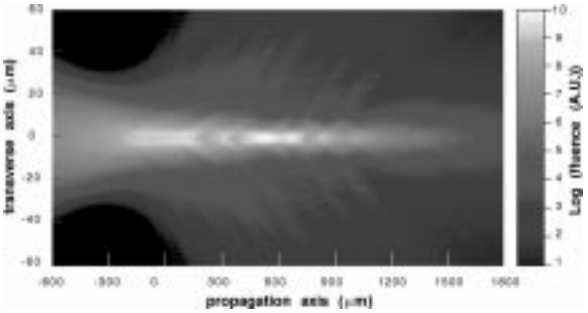

Fig. 2. Base 10 logarithm of the two-dimensional pulse fluence for a relativistic intensity of $I = 3 \times 10^{18}$ W/cm^2. Laser pulse propagates is from left to right. The focal plane in vacuum corresponds to the position $z = 0$. The peak fluence is 2.5 times the peak value in vacuum. Like in all the simulations presented here a cylindrical symmetry is assumed.

interaction experiment at moderate intensities where thermal self-focusing was detected using picosecond resolution soft X-ray imaging of the laser-plasma interaction region [12].

In this paper we present numerical simulations of the relativistic heating of an underdense plasma which show that the properties of the resulting electron distribution function meet the conditions required for an experimental investigation based on soft X-ray techniques. These studies have been performed with the particle code WAKE [13,14] that allows cylindrically symmetric or Cartesian 2D simulations of the relativistic interaction of a short laser pulse with an underdense plasma to be performed in the quasi-static, large-band paraxial approximation. The code also includes tunnel ionisation of the gas medium and accounts for ionisation defocusing effects. The performance of the code with respect to the physics of relativistic laser-plasma interactions has been carefully tested and its reliability was confirmed by the successful design and interpretation of laser-plasma experiments in the relativistic wake-field [3] and tunnel ionisation regimes [15].

The interaction conditions considered in our simulations are based on laser parameters presently available in high power laser facilities. The code WAKE was run in cylindrical geometry using a 1.054 μm wavelength, 700 fs FWHM pulse focused into a gas-jet target in a waist of radius $w_0 = 10$ μm, and a Rayleigh length $z_0 = 300$ μm. The laser intensity I was varied between 4×10^{17} and 1.2×10^{19} W/cm^2. The target medium parameters chosen in our simulations are consistent with a typical gas-jet target experiment. In particular, the atomic density was homogeneous in the transverse direction x and Gaussian in the longitudinal direction z with a peak atomic density, $N_{\max} = 10^{19}$ cm^{-3} and FWHM length $L = 1.2$ mm. In order to fully describe ionisation effects, helium was assumed in our simulations. However, as discussed below, higher Z gases like neon and argon, could be a better choice if a brighter X-ray emission in a specific spectral region is required. The pulse is focused at the position where the gas density is one half of the maximum density. This focal position was chosen in order to minimise the defocusing effects arising from gas ionisation and maximise self-guided propagation. It was tested that ionisation defocusing was negligible in this case.

The laser energy losses taking place at intensities below and just above $a_0 = 1$ are compared in Figure 1. The e.m. wave energy E reaching the plane $z = const$, integrated over the full laser pulse duration, is plotted as a function of the co-ordinate z along the optical axis for a moderately relativistic peak intensities of 3×10^{18} W/cm^2 (solid line) which corresponds to $a_0 \approx 1.5$. The corresponding curve for the case of non-relativistic, but highly non-linear regime, obtained at a laser intensity of 4×10^{17} ($a_0 \approx 0.5$) is also shown for comparison (dashed line). The energy E is normalised to $E_{\rm tot}$ which is the total pulse energy delivered by the laser system. A more comprehensive view of the e.m. wave propagation process for the moderately relativistic peak intensity ($I = 3 \times 10^{18}$ W/cm^2) is given in Figure 2 which shows the logarithm of the two-dimensional pulse fluence spatial distribution ($F(x,z) = \int I(x,z)\mathrm{d}t$).

According to the results of Figure 1, laser absorption increases dramatically as the laser intensity enters the relativistic regime. In fact, after passing through the plasma the laser beam energy is reduced to less than 10%, while no significant energy escapes through the simulation borders, as shown by the fluence distribution of Figure 2. This absorption is a typical relativistic effect and disappears, as the pulse peak intensity is decreased (dashed line). It is clear from the fluence distribution of Figure 2 that the e.m. energy is concentrated around the optical axis and exhibits the characteristic behaviour of the oscillating self-focusing. These oscillations are clearly shown by the lineout of Figure 3, which gives the fluence on the axis as a function of the axial co-ordinate. This behaviour is related to the self-modulation of the laser pulse into very short sub-pulses *via* the excitation of a wake-field. Due to the non-uniform electron density along the gas-jet, and to the pulse focusing, these sub-pulses become, after some propagation, very irregular in duration and intensity. A similar behaviour was found in the laser intensity along the transverse co-ordinate for different positions along the propagation axis.

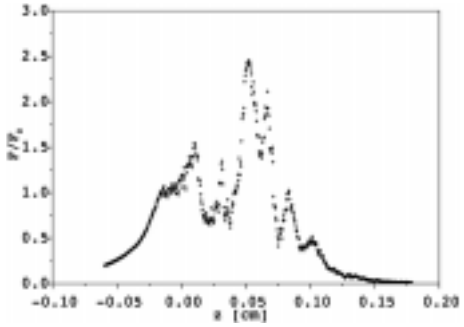

Fig. 3. Lineout of the fluence distribution of Figure 2 along the optical axis ($x = 0$) showing the characteristic behaviour of the oscillating self-focusing related to the self-modulation of the laser pulse into very short sub-pulses.

As discussed above, a crucial issue in relativistic laser-plasma interactions is the energy transfer from the laser pulse to the electrons and the ions of the plasma. From an experimental viewpoint, the problem can be investigated for example, by means of optical probing and time/space resolved X-ray emission measurements. Optical probing can provide information on the electron density distribution while X-ray diagnostics can be very sensitive to localised energy deposition which gives rise to changes of electron temperature and/or density in the plasma. As shown above, these are the typical effects produced by relativistic self-focusing.

In order for X-ray diagnostics to be effective, the temporal resolution must be sufficient to discriminate between the short (< 1 ps) interaction time and the subsequent evolution of the plasma which may require up to tens of picosecond. On the other hand, the spatial resolution of X-ray imaging must be sufficient to resolve the typical scalelength of localised energy deposition in the plasma which, in the presence of self-focusing, can be as small as a few micrometers. These requirements can only be met in the soft X-ray region, say for photon energies around 2–3 keV, where measurements with such an accuracy can be performed. On the other hand, these photons are typically generated by the so-called *thermal* electrons *via* collisional processes. Therefore, for soft X-ray diagnostics to be effective, a substantial fraction of the laser energy must be transferred to these *thermal* electrons.

This problem has been studied directly in our simulations looking at the electron distribution function. A measure of the *thermalisation* of electrons can be obtained by comparing the integrated spectrum from zero to say 2 keV to the total integral spectrum. According to our simulations the fraction of energy in the low-energy region is typically greater than 15% of the total electron energy. In particular, the electron energy distribution function obtained from our simulations at $I = 3 \times 10^{18}$ W/cm^2 is shown in Figure 4a for different positions along the z-axis. These plots show that the shape of the electron energy spectrum below 2 keV depends strongly upon the position along the propagation axis and peaks always around a few hundreds of electron-volts. Also, most of the electrons with energy of about 1 keV are produced just after laser radiation has

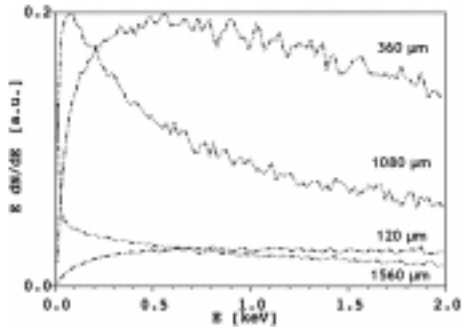

(a)

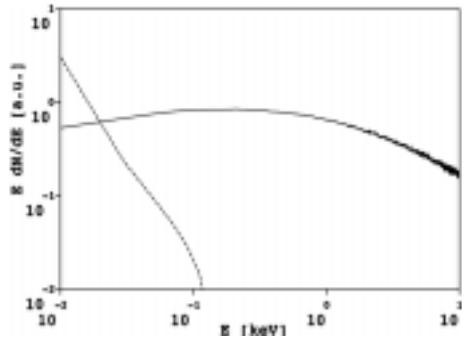

(b)

Fig. 4. (a) Electron energy distribution for different positions along the z-axis, from $z = 120$ μm, to $z = 1560$ μm. The spectra are integrated from $t = -\infty$ up to $t = 1$ ps after the pulse peak. (b) Electron spectra for the two laser intensities of 3×10^{18} (solid line) and for 4×10^{17} (dashed line). These curves give the total electron energy spectra for energies up to 10 keV, taken after the passage of the laser pulse and integrated (along z) over the entire plasma column.

overcome the plasma density maximum, where the density is decreasing.

Another signature of the dramatic change of energy transfer efficiency with the laser intensity can also be found comparing the integral electron spectra plotted in Figure 4b for the two laser intensities of 3×10^{18} (solid line) and for 4×10^{17} (dashed line). These curves give the total electron energy spectra for energies up to 10 keV, taken after the passage of the laser pulse and integrated along z over the entire plasma column. As expected, in the lower intensity case, very little energy is transferred to the electrons whose typical kinetic energy is below the 100 eV region. In contrast, in the higher intensity case the total energy transferred to the electrons is approximately hundred times higher. The heated electrons have a typical energy of several hundreds of eV with an important fraction of electrons having an energy above 1 keV. These results confirm that, although the intense laser light will accelerate some electrons to extremely high energies as already observed in other simulations [16], a considerable fraction of the laser energy is transferred to thermal electrons.

Further insight in the self-focusing dynamics can be obtained from the electron and ion density map and their temporal evolution. Figure 5 shows the temporal evolution of the electron density profile along the

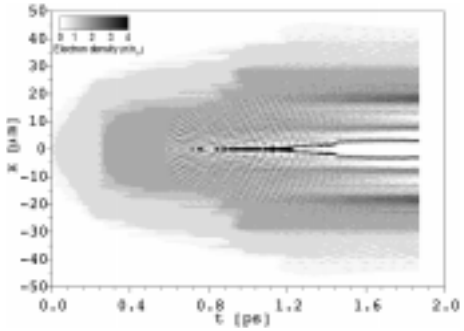

Fig. 5. Temporal evolution of the electron density profile along the transverse co-ordinate x at the position of the best focus in vacuum ($z = 0$), for a laser intensity of 3×10^{18} W/cm^2.

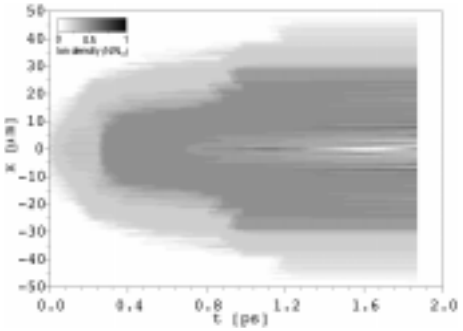

Fig. 6. Temporal evolution of the ion density profile along the transverse co-ordinate x at the position of the best focus in vacuum ($z = 0$), for a laser intensity of 3×10^{18} W/cm^2.

transverse co-ordinate x at the position of the best focus in vacuum ($z = 0$). Electron density modulations of the same scalelength as in the intensity plot of Figure 2 are present in the distribution of Figure 5. Other features, like a channel, about 10 μm in diameter, can also be found in the plot of Figure 6 which shows the temporal evolution of the ion density profile. The channel originates from the ponderomotive expulsion of electrons from the underdense plasma.

The scenario described for moderately relativistic laser pulses is basically unchanged if the laser intensity is further increased to the highly relativistic regime. In fact, simulations performed with a peak vacuum intensity of 1.2×10^{19} W/cm^2 ($a_0 \approx 3$) show large energy deposition, and electrons in the region below 2 keV still holding at least 10% of the total electron energy. The development of an ion channel, immediately after the e.m. pulse has passed, is also seen in the simulations and the density at the boundaries of the channel was found to be more than twice the background density. All these results are very promising in terms of the possibility of using X-ray diagnostics to investigate absorption processes and self-focusing in relativistic laser-plasma interactions.

We also studied the case of laser interaction with pre-formed plasmas, an alternative to gas-jets in this class of experiments. In fact, well characterised, uniform test plasmas can be obtained with the well established exploding foil technique [10,11]. In contrast with the case of interaction with a gas-jet, in this case the plasma is assumed to be pre-ionised. This may result in a different initial behaviour if processes like ionisation defocusing were important in the case of a gas-jet. Our simulations in underdense pre-formed plasmas were found to be very much similar to those obtained for interaction with gas-jets from the point of view of total energy deposition as well as from the point of view of propagation related processes.

In conclusion, we studied the interaction of a relativistic laser pulse with a gas-jet using numerical simulations. A crucial aspect of this class of experiments is the relationship between the energy loss of the laser pulse and the energy gain of electrons and ions. Our simulations show a clear enhancement of the laser energy deposition in an underdense plasma with increasing laser intensity when the relativistic regime is approached. The energy is released in a region very close to the laser beam axis. Even though a number of electrons are accelerated to extremely high energies, a considerable fraction of the laser energy is transferred to thermal electrons. There is also a clear evidence of channel formation at the end of the pulse.

An experiment is possible in which these features can be studied by means of time and space-resolved detection of soft X-rays combined with interferometric measurement of the time evolution of the density channel and calorimetry of the transmitted laser pulse. These measurements are also expected to give direct evidence, if any, of relativistic self-focusing and self-guiding, issues which are of great relevance for the fast ignitor approach to inertial confinement fusion.

References

1. B. Langdon, Phys. Rev. Lett. **44**, 575 (1980).
2. A. Djaoui, A. Offenberger, Phys. Rev. E **50**, 4961 (1994).
3. P. Chessa, P. Mora, T.M. Antonsen Jr, Phys. Plasmas **5**, 3451 (1998).
4. J.C. Adam, A. Héron, S. Guérin, G. Laval, P. Mora, B. Quesnel, Phys. Rev. Lett. **78**, 4765 (1997).
5. K. Krushelnick *et al.*, Phys. Rev. Lett. **83**, 737 (1999).
6. M. Borghesi, A.J. Mackinnon, R. Gaillard, O. Willi, A. Pukhov, J. Meyer-ter-Vehn, Phys. Rev. Lett. **80**, 5137 (1998).
7. S.Y. Chen, G.S. Sarkisov, A. Maksimchuk, R. Wagner, D. Umstadter, Phys. Rev. Lett. **80**, 2610 (1998).
8. J.A. Cobble, R.P. Johnson, R.J. Mason, Phys. Plasmas **5**, 4005 (1998); P.E. Young, P.R. Bolton, Phys. Rev. Lett. **77**, 4556 (1996).
9. L.A. Gizzi, D. Giulietti, A. Giulietti, T. Afshar-Rad, V. Biancalana, P. Chessa, E. Schifano, S.M. Viana, O. Willi, Phys. Rev. E **49**, 5628 (1994).
10. M. Borghesi, A. Giulietti, D. Giulietti, L.A. Gizzi, A. Macchi, O. Willi, Phys. Rev. E **54**, 6769 (1996).
11. L.A. Gizzi, A. Giulietti, O. Willi, J. X-ray Sci. Technol. **7**, 186 (1997).
12. T. Afshar-Rad, L.A. Gizzi, M. Desselberger, F. Khattak, O. Willi, A. Giulietti, Phys. Rev. Lett. **68**, 942 (1992).
13. T.M. Antonsen Jr, P. Mora, Phys. Fluids B **5**, 1440 (1993).
14. P. Mora, T.M. Antonsen Jr, Phys. Plasmas **4**, 217 (1997).
15. P. Chessa, E. De Wispelaere, F. Dorchies, G. Hamoniaux, V. Malka, J.R. Marquès, F. Amiranoff, A. Antonetti, P. Mora, Phys. Rev. Lett. **82**, 552 (1999).
16. A. Pukhov, J. Meyer-ter-Vehn, Phys. Rev. Lett. **76**, 3975 (1996).